Sheet metal forming limits as classification problem

Christian Jaremenko[1], Xiaolin Huang[1], Emanuela Affronti[2], Marion Merklein[2], Andreas Maier[1]
[1]Pattern Recognition Lab, [2]Institute of Manufacturing Technology
Friedrich-Alexander-University Erlangen-Nuremberg, Erlangen, Germany
christian.jaremenko@fau.de

Abstract

Forming limit diagrams are used to evaluate the formability of metal sheets and describe the maximum strain to failure in terms of major and minor strain. The main idea is the detection of the onset of necking in limited areas of the investigated sheet metals. Current methods introduce location- or time-dependency or may require user interaction. Within this contribution we interpret the onset of necking as classification problem and show that a support vector machine performs comparable to a human experts group. Best results reach up to 87.5 % avg. precision and 84.9 % avg. recall, using all available 2D-information, while being time- and location-independent.

1 Introduction

Climate change, increasing price of raw materials and legal requirements encourage the automotive industry to produce vehicles with reduced emission and fuel consumption. One possibility to realize these goals is to reduce the weight of their upcoming product generations and thus the substitution of conventional steelworks with high-strength and lightweight material. In comparison with conventional deep drawing steelworks, high-strength lightweight materials often have a lower forming capacity due to their different material properties. To investigate the feasibility of the production of components, numerical simulation methods e.g. finite element analysis are taken into account. These forming simulations are used to predict the failure probability and thus highly depend on a failure criterion that identifies the maximum forming capacity of sheet metals. This criterion is either described by the local thinning in the direction of the sheet thickness or by the cancellation of the material composite in form of a crack. The forming limit diagram (FLD) considers both criteria and is an established method excessively used within finite element analysis. Forming limit analysis was introduced by Keeler [1] in 1963 and to this day the onset of necking leading to crack initiation is considered as the forming limit of sheet metals, denoted by the forming limit curve (FLC) within the FLD. Current established methods [2, 3, 4] use an optical strain measurement system based on digital image correlation (DIC) to determine the FLC, while sharing some disadvantages. The standardized evaluation method [2] is position-dependent and does not consider the strain development over time. The time-dependent methods by Merklein et al. [3] and Volk and Hora [4] consider the strain development over time, but are limited regarding their evaluation area. Volk and Hora define the onset of necking as a sudden change of thickness reduction in the critical area and as consequence do not incorporate the development of the material structure outside of the investigated area. This is disadvantageous especially in case of materials with abrupt fracture behavior, as potentially valuable information is missed and thus may lead to wrong forming limits. Aside from this the time-dependent methods introduce a high variance for the forming limit as they are dependent on the acquisition rate of the strain measurement system.
This paper introduces and discusses a classification approach to alternatively define the forming limit curve. The main difference in comparison with state of the art methods is the incorporation of expert knowledge as well as the evaluation of the complete image data, besides being time- and location-independent. In addition, a comparison between the experts group and the classification approach is performed to evaluate the feasibility of automation.

2 Related Work

The forming limit describes the maximum strain to failure in dependence of major strain (ε_1) and minor strain (ε_2), while major strain defines the direction of largest deformation and minor strain is perpendicular to it. In this context, strain is defined by the relative elongation of a chassis under load conditions $e = \frac{\Delta l}{l_0}$, where l_0 denotes the original length and Δl the deviation length. This can be reformulated to true strain $\varepsilon = \ln(1 + e)$. Thinning (ε_3) in the direction of sheet metal thickness reduction can only be determined indirectly by exploiting the law of volume constancy ($0 = \varepsilon_1 + \varepsilon_2 + \varepsilon_3$) [5].
The FLC can be determined experimentally following a Nakazima or Marcinak test setup under laboratory like conditions as standardized in [2]. Both test setups are based on the same idea. The sheet metal is clamped into a blank holder and deformed until fracture by applying load with a punch. Beforehand the examined sheet metals are prepared with a speckle pattern, digitally subdivided into small rectangular areas and tracked during the forming procedure using an optical measurement system in combination with a DIC approach. The displacements between subsequent images are used to calculate the principal strains and visualized as 2-D strain distributions as $\varepsilon_1 - \varepsilon_3$ in Fig. 1. The onset of necking is the local concentration of remaining plastic deformation in small bands and a fallback of the remaining areas in the elastic range. The strain inside these bands increases over time while it remains constant outside as visualized in Fig. 1. To determine the complete FLC multiple specimen with a variety of cutouts from the sheet metal (S30 - S245) are investigated to simulate different strain states, ranging from uniaxial stretching ($\varepsilon_1 = -2\varepsilon_2$) over plane strain ($\varepsilon_2 = 0$) to biaxial stretching ($\varepsilon_1 = \varepsilon_2$), whereby the resulting forming limit per strain state is defined by

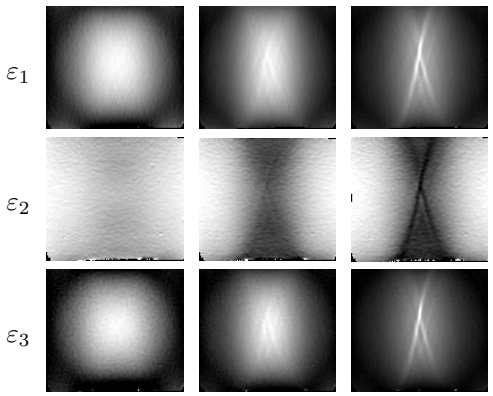

Figure 1. Strain progression (left to right) and localization effect of $\varepsilon_1 - \varepsilon_3$ during forming.

the average of three trials. The international standard [2] describes the intersection line method to determine the FLC. This method uses the major- and minor strain values along a virtual intersection line in the 2-D strain distribution through the maximum major strain value, perpendicular to crack progression. This procedure clearly introduces location dependence that is partly addressed by performing multiple sections. To improve the predictability of the onset of necking new methods were introduced taking the forming history into account. Merklein et al. [3] and Volk and Hora [4] follow comparable approaches, investigating limited areas of different principal strains. Merklein et al. evaluate ε_1 information, whereas Volk and Hora examine ε_3. Both methods use the last frame before crack occurrence to define the evaluation area. Afterwards the complete forming procedure is re-investigated using this defined and averaged area. The necking criterion introduced by Volk and Hora is visualized in Fig. 2. To define the forming limit, the thinning rate, the first derivative of the deformation in ε_3 direction, is evaluated. Two straight lines are fitted into the homogeneous and instable forming region, while their intersection depicts the onset of plastic instability and the related ε_1 and ε_2 values define the forming limit. Aside from the evaluation area size, the quality of the estimates of the intersection lines is dependent on the amount of available points and thus dependent on the acquisition rate. Two FLCs of AC170 aluminum alloy obtained using the described methods are shown in Fig. 3 with the forming history of one uniaxial strain state (S60). The general shapes of the FLC seem comparable, but large deviations between individual strain states are apparent indicating that current methods are approximations of varying quality. Vysochinskiy et al. [6] introduced the thickness-ratio to define the onset of necking, that compares single point with limited area effects, in combination with user interaction. Only Vacher et al. [7] exploit complete images by using the strain velocity, the difference between two subsequent ε_1 distributions, to determine the onset of instability without defining a concrete necking criterion. A first attempt to introduce pattern recognition methods in forming analysis was introduced by Merklein et al. [8], as they used multiple random strain values of ε_1–ε_3 in a random forest regression experiment to predict the onset of fracture. Beside the approach of

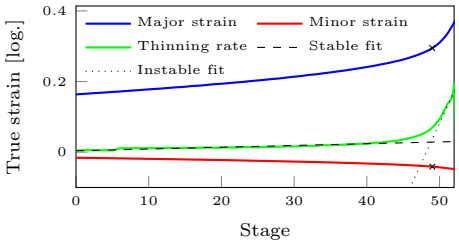

Figure 2. Onset of necking according to Volk and Hora [4].

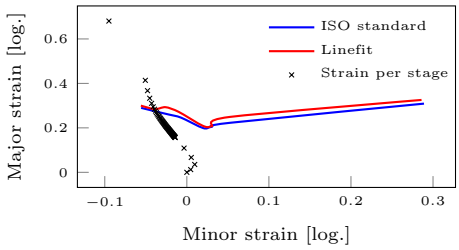

Figure 3. Different forming limit curves with AC170-S60 strain path forming history.

Vacher et al., all of the mentioned methods share the similarity that only limited parts of the available information is considered and that user interaction in terms of thresholds or prior-knowledge is required. Possible effects that occur outside the evaluation area or the investigated principal strain are neglected. Thus it may be beneficial to incorporate the whole image information ($\varepsilon_1 - \varepsilon_3$) rather then restricting the evaluation to one of the principal strains with limited investigation area. To avoid the time- and location dependency, expert knowledge is used to describe the forming behavior and the onset of instability.

3 Materials and Methods

Nakajima Test Setup. A Nakajima testing machine was used for the present investigation. Fig. 4 shows the scheme of the test setup as well as the investigated sample geometry. A sample, clamped in between the blank holder and the die, is formed until fracture by a punch progressing in vertical direction. The forming procedure is evaluated with a two CCD-camera setup, using the optical strain measurement system Aramis (GOM). A high-strength lightweight aluminum alloy AC170 is selected as specimen material with a sheet thickness of 1 mm. To generate the data set three trials of the S60 geometry were performed with a constant punch velocity of 1 mm/s and a sampling rate of 15 Hz.

Expert Interviews. Each of the three trials were evaluated by four experts of the Institute of Manufacturing Technology of the Friedrich-Alexander-University Erlangen-Nuremberg. Within each video sequence the individual frames of the strain distributions are labeled, based on visual impressions, with four different classes, namely in-suspicious (C0), diffuse necking (C1), local necking (C2) and crack initiation (C3). The mean and standard deviation of the experts decisions are visualized in Fig. 5. A majority scheme is enforced to realize distinct transitions be-

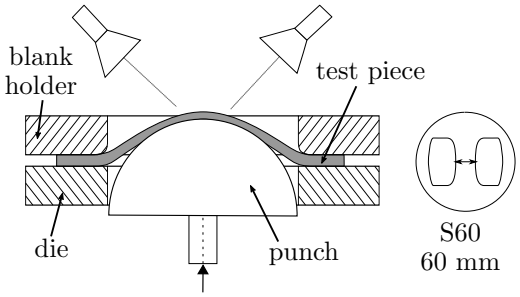

Figure 4. Nakajima test setup with S60 geometry.

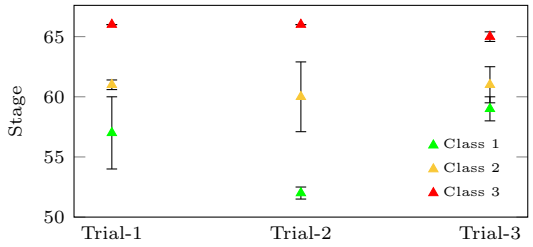

Figure 5. Beginning of classes (stage in time) according to experts with standard deviation.

tween the individual classes. As the amount of experts is four, the decision in case of parity is made in favor of the higher class. The distributions of classes within each trial is depicted in Tab. 1.

Feature Extraction & Classification. The decisions of the experts are based on visual impressions. This indicates that contrast changes, inhomogeneities as well as edges are important within the process of decision-making. Jaremenko et al. [9] solve a comparable classification problem, despite the different image characteristic, based on the evaluation of inhomogeneities. Hence, local binary patterns (LBP) [10] and gray level co-occurrence matrices (GLCM) [11] serve as features extracted from $\varepsilon_1 - \varepsilon_3$. Multiple radii (1, 3, 5) and neighborhoods (8, 16, 24) are chosen in case of the rotation invariant LBPs following a multiscale approach. In case of the GLCM multiple distances are combined ranging from 1 to 5. As a result of the heavy data imbalance, the classification problem is solved in a hierarchical manner based on support vector machines [12], that was showing superior performance in preliminary studies in comparison with a one vs all approach. Therefore three binary classification problems are solved sequentially based on the outcome of the previous classification stage.

4 Experiments

The inter-experts consistency is measured with a "Leave-One-Expert-Out Cross-Validation" (LOEO-CV) based on the assigned labels per trial. A majority voting scheme of the expert decisions of each individual trial provides the labels used in the classification procedure. The performance of the classifier is determined based on "Leave-One-Sequence-Out Cross-Validation" (LOSO-CV) experiments, while three different feature-extraction methods are evaluated and compared. The "PS-AVG" experiment uses rectangular-patches with a side length of 25 pixels and 50% overlap with subsequent averaging and calculation of the standard deviation over all patches and features. The "FI" experiment evaluates the whole image without subdivision into patches. In case of the "PS-25" experiment the averaging step is skipped, that leads to a large location-dependent feature vector. All experiments are evaluated using precision and recall as evaluation measure.

Table 1. Class support – Majority.

Class	C0	C1	C2	C3
Trial-1	51	5	4	1
Trial-2	47	6	7	1
Trial-3	54	1	5	1
Total	152	12	16	3

Table 2. Overall expert consent (in %).

	C0	C1	C2	C3	Precision	Recall
C0	95.8	3.4	0.8	0.0	96.1	95.8
C1	59.0	25.6	15.4	0.0	21.7	25.6
C2	1.7	25.9	72.4	0.0	77.8	72.4
C3	0.0	0.0	7.7	92.3	100.0	92.3
Mean					73.9	71.5

Table 3. Classification results (in %) – PS-25.

	C0	C1	C2	C3	Precision	Recall
C0	100.0	0.0	0.0	0.0	98.7	100
C1	16.7	58.3	25.0	0.0	70.0	58.3
C2	0.0	18.7	81.3	0.0	81.3	81.3
C3	0.0	0	0.0	100.0	100	100
Mean					87.5	84.9

5 Results

The results of the LOEO-CV experiment is visualized in Tab. 2. Overall an avg. precision of 73.9 % and avg. recall of 71.5 % is achieved. The best consensus is reached within C0 and C3 with 96.1 % and 100 % precision, respectively. Good consensus of 77.8 % is achieved in C2, while a low consent of 21.7 % between the experts prevails in C1. Within all LOSO-CV experiments, the LBP features consistently slightly outperformed the GLCM features. Therefore only the LBP feature results of the different experiments are visualized in Tab. 3-5. Best results in terms of avg. recall and avg. precision are achieved with the PS-25 (87.5 %,84.9 %) experiment, outperforming the PS-AVG (79.5 %, 82.0 %) and FI (80.7 %, 82.0 %) experiment. Differences exist within the individual class recognition rates. The PS-AVG and FI method have advantages classifying C2 and C3 as precision and recall reach 88.9 %, 100 % and 94.1 %,100 and 100 %, 100 %, respectively. In case of C1 only 33.3 % and 33.3 % precision and recall are achieved. The PS-25 method outperforms the other approaches in case of C0 and C1, especially within C1 as it reaches 70 % precision and 58.3 % recall, while it performs worse in case of C2 with 81.3 % for both measures.

6 Discussion and Conclusion

The LOEO-CV experiment highlights the consent between the individual experts. Very good consistency

Table 4. Classification results (in %) – PS-AVG.

	C0	C1	C2	C3	Precision	Recall
C0	94.7	5.3	0.0	0.0	96.0	94.7
C1	50.0	33.3	16.7	0.0	33.3	33.3
C2	0.0	0.0	100.0	0.0	88.9	100
C3	0.0	0.0	0.0	100.0	100	100
Mean					79.5	82.0

Table 5. Classification results (in %) – FI.

	C0	C1	C2	C3	Precision	Recall
C0	94.7	5.3	0.0	0.0	95.4	94.7
C1	58.3	33.3	8.3	0.0	33.3	33.3
C2	0.0	0.0	100.0	0.0	94.1	100
C3	0.0	0.0	0	100.0	100	100
Mean					80.7	82.0

is achieved in C0, C2 and C3. Especially in case of C3 this was to be expected as the crack occurs very abruptly on the last stage of the sequence. The localization effect as well as the in-suspicious class is recognized by all experts with good consent as precision and recall emphasize. Diffuse necking seems to be more difficult to recognize, as the low values of the evaluation measures indicate. This results from inconsistencies between expert opinions and the fact that not all experts were able to identify a diffuse necking state for this material and geometry.
The output of the classifiers are hard decision based on the majority voting of all human experts. The same difficulties in distinguishing C1 from the other classes can be seen within the classification results of PS-AVG and FI, as most of the missclassifications occur between C0 and C1. Both methods are location-independent due to the analysis of either the whole image or the averaging scheme. As nearly 50 % of the instances of C1 are missclassified as C0 and C2, this might indicate that diffuse necking is a very short phase of the forming procedure or that one of the three trials behaves differently in comparison with the rest. One candidate for this misbehavior is trial-3 as indicated by the majority scheme with the low amount of C1 members. When location dependence is maintained, the classification of C0 and C1 improve with the PS-25 method. Nevertheless, the classification of C1 still performs worse while the precision and recall nearly double. As a downside the precision and recall of C2 decreases as missclassifications between C1 and C2 increase. The localization effect of the sheet metal as well as the crack initiation can be identified nearly perfect with the location-independent PS-AVG and FI method as emphasized by the classification results of C2 and C3. Both methods do not confuse any instance of C2 with other classes. This is advantageous as C2 would be the most significant class in forming processes as it describes the localization effect and thus the missclassifications in C0 and C1 may be tolerated. Currently all instances are processed with the same importance and none of the classes is preferred over the other with a weighting scheme. Of course a certain amount of subjectivity is introduced and addressed by using the knowledge of multiple experts. Another aspect that needs further investigation is the exact area definition of the onset of necking in terms of major and minor strain. This would enable a comparison with state of the art methods, as up to now only the point in time during forming processes is determined.
A new concept for the determination of the FLD is presented in this contribution. It is defined as classification problem evaluating $\varepsilon_1 - \varepsilon_3$. The definition of the necking phase relies on expert knowledge instead of approximations based on thinning or strain rates of limited areas. This makes it applicable to define the necking effect in terms of $\varepsilon_1 - \varepsilon_3$. In combination with the classification approach a transfer of knowledge on comparable materials seems feasible. This would allow a definition of the forming limit in terms of principal strain and feature space. In future work this approach is extended on the complete FLD with investigation of multiple materials.

References

[1] S.P. Keeler and W. A. Backofen. Plastic instability and fracture in sheets stretched over rigid punches. *Trans. Asm*, 56(1):25–48, 1963.

[2] ISO12004-2:2008. Metallic Materials Sheet and Strip Determination of Forming-Limit Curves. Part 2: Determination of Forming-Limit Curves in the Laboratory, 2008.

[3] M. Merklein, A. Kuppert, and M. Geiger. Time dependent determination of forming limit diagrams. *CIRP Annals - Manufacturing Technology*, 59(1):295–298, 2010.

[4] W. Volk and P. Hora. New algorithm for a robust user-independent evaluation of beginning instability for the experimental FLC determination. *Int. J. Mater. Form.*, 4(3):339–346, 2011.

[5] D. Banabic. *Sheet Metal Forming Processes*. Springer Berlin Heidelberg, 2010.

[6] D. Vysochinskiy, T. Coudert, O.S. Hopperstad, O.G. Lademo, and A. Reyes. Experimental detection of forming limit strains on samples with multiple local necks. *J. Mater. Process. Technol.*, 227:216–226, 2016.

[7] P. Vacher, A. Haddad, and R. Arrieux. Determination of the Forming Limit Diagrams Using Image Analysis by the Corelation Method. *CIRP Annals - Manufacturing Technology*, 48(2):227–230, 1999.

[8] M. Merklein, A. Maier, D. Kinnstätter, C. Jaremenko, and E. Affronti. A New Approach to the Evaluation of Forming Limits in Sheet Metal Forming. *Key Eng. Mater.*, 639:333–338, 2015.

[9] C. Jaremenko, A. Maier, S. Steidl, J. Hornegger, N. Oetter, C. Knipfer, F. Stelzle, and H. Neumann. Classification of Confocal Laser Endomicroscopic Images of the Oral Cavity to Distinguish Pathological from Healthy Tissue. In *Bildverarbeitung für die Medizin*, pages 479–485. Springer Berlin Heidelberg, 2015.

[10] T. Ojala, M. Pietikainen, and T. Maenpaa. Multiresolution gray-scale and rotation invariant texture classification with local binary patterns. *IEEE Trans. Pattern Anal. Mach. Intell.*, 24(7):971–987, 2002.

[11] R.M. Haralick, K. Shanmugam, and I. Dinstein. Textural Features for Image Classification. *IEEE Trans. Syst. Man Cybern.*, 3(6):610–621, nov 1973.

[12] J. Platt. Sequential minimal optimization: A fast algorithm for training support vector machines. Technical report, Microsoft Research, 1998.